CHAPTER 2

Examination of the contributions of size and avidity to the neutralization mechanisms of the anti-HIV antibodies b12 and 4E10

Published as Klein JS, Gnanapragasam PNP, Galimidi RP, Foglesong CP, West AP, Jr., and Björkman PJ (2009) Examination of the contributions of size and avidity to the neutralization mechanisms of the anti-HIV antibodies b12 and 4E10. *Proc Natl Acad Sci U S A.* **106**:7385-90.

Examination of the contributions of size and avidity to the neutralization mechanisms of the anti-HIV antibodies b12 and 4E10

Joshua S. Klein[a], Priyanthi N. P. Gnanapragasam[b], Rachel P. Galimidi[b], Christopher P. Foglesong[b], Anthony P. West, Jr.[b], and Pamela J. Bjorkman[b,c,1]

[a]Graduate option in Biochemistry and Molecular Biophysics, [b]Division of Biology, [c]Howard Hughes Medical Institute, California Institute of Technology, Pasadena, CA 91125

Edited by Stephen C. Harrison, Children's Hospital Boston, Boston, MA, and approved March 10, 2009 (received for review November 11, 2008)

Monoclonal antibodies b12 and 4E10 are broadly neutralizing against a variety of strains of the human immunodeficiency virus type 1 (HIV-1). The epitope for b12 maps to the CD4-binding site in the gp120 subunit of HIV-1's trimeric gp120-gp41 envelope spike, whereas 4E10 recognizes the membrane-proximal external region (MPER) of gp41. Here, we constructed and compared a series of architectures for the b12 and 4E10 combining sites that differed in size, valency, and flexibility. In a comparative analysis of the ability of the b12 and 4E10 constructs to neutralize a panel of clade B HIV-1 strains, we observed that the ability of bivalent constructs to cross-link envelope spikes on the virion surface made a greater contribution to neutralization by b12 than by 4E10. Increased distance and flexibility between antibody combining sites correlated with enhanced neutralization for both antibodies, suggesting restricted mobility for the trimeric spikes embedded in the virion surface. The size of a construct did not appear to be correlated with neutralization potency for b12, but larger 4E10 constructs exhibited a steric occlusion effect, which we interpret as evidence for restricted access to its gp41 epitope. The combination of limited avidity and steric occlusion suggests a mechanism for evading neutralization by antibodies that target epitopes in the highly conserved MPER of gp41.

HIV type 1 (HIV-1) is an enveloped virus that presents severe challenges to eliciting effective antibody-mediated immune responses because it employs multiple strategies to evade antibodies. The virus rapidly mutates to change residues on its surface (1), conceals other potential antibody epitopes with carbohydrates (2), hides conserved regions at interfaces by oligomerization, and prevents access to conserved regions by conformational masking and steric occlusion (2–5). Despite these escape mechanisms, a limited number of broadly neutralizing antibodies have been isolated from HIV-1-infected individuals over the past few decades (reviewed in ref. 6). They target well-defined epitopes on both subunits of the HIV-1 envelope spike, a trimeric complex composed of 3 copies of 2 noncovalently associated glycoproteins, gp120 and gp41. One such antibody called b12 binds to an epitope that overlaps the host receptor (CD4)-binding site on gp120 (7, 8), and another called 4E10 binds to an epitope in the highly conserved membrane proximal external region (MPER) of gp41 (9–12). Both antibodies were shown to be broadly neutralizing across a diverse panel of HIV-1 strains, although 4E10 exceeded b12 in the breadth of its reactivity (13).

The neutralization potency of an antibody against a virus can be improved by orders of magnitude through the effects of avidity (14–18). The term avidity in the context of antibodies refers to their ability to simultaneously bind 2 physically linked antigens (e.g., 2 spikes on the surface of the same virus) by using the 2 identical combining sites located at the tips of their Fab (antigen-binding fragment) arms (19) (Fig. 1). In order for avidity to occur, the antigen sites must be present at sufficient density such that once the first Fab has bound, the second Fab can bind its partner before the first Fab dissociates. The number of spikes on HIV-1 is ≈15 per virion (20–23), whereas ≈450 spikes per virion have been observed on the similarly sized influenza type A virus (24). The extent to which the relatively low density of HIV-1 envelope spikes might impact the avidity of anti-HIV-1 antibodies is not yet understood.

Our objective in the present study was to ask how the difference between monovalence and bivalence coupled with

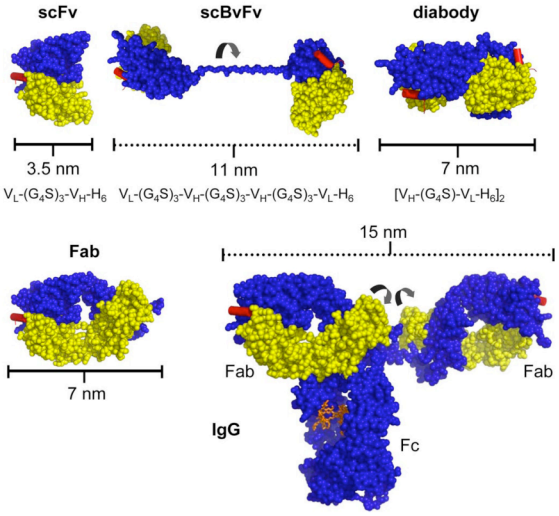

Fig. 1. Structures of antibody constructs. Space-filling models are presented above a description of the domain organization for each construct (V_L, variable light; V_H, variable heavy; (G_4S), Gly-Ser linker; H_6, 6×-His tag). Models were constructed by using coordinates for the heavy (blue) and light (yellow) chains of Fab 4E10 and its peptide epitope (red) (PDB ID code 1TZG) (34). For the diabody model, 2 4E10 V_H–V_L pairs were aligned to the structure of diabody L5MK16 (PDB ID code 1LMK) (30). For the IgG model, 2 4E10 Fabs were used to replace the b12 Fabs in the structure of intact IgG1 b12 (PDB ID code 1HZH) (55). Solid lines indicate approximate dimensions for the scFv, diabody, and Fab. Dotted lines indicate approximate maximal distances between combining sites for the scBvFv and IgG. Curved black arrows indicate axes of rotation.

Author contributions: J.S.K., A.P.W., and P.J.B. designed research; J.S.K. and P.N.P.G. performed research; J.S.K., R.P.G., and C.P.F. contributed new reagents/analytic tools; J.S.K., P.N.P.G., A.P.W., and P.J.B. analyzed data; and J.S.K. and P.J.B. wrote the paper.

The authors declare no conflict of interest.

This article is a PNAS Direct Submission.

[1]To whom correspondence should be addressed. E-mail: bjorkman@caltech.edu.

This article contains supporting information online at www.pnas.org/cgi/content/full/0811427106/DCSupplemental.

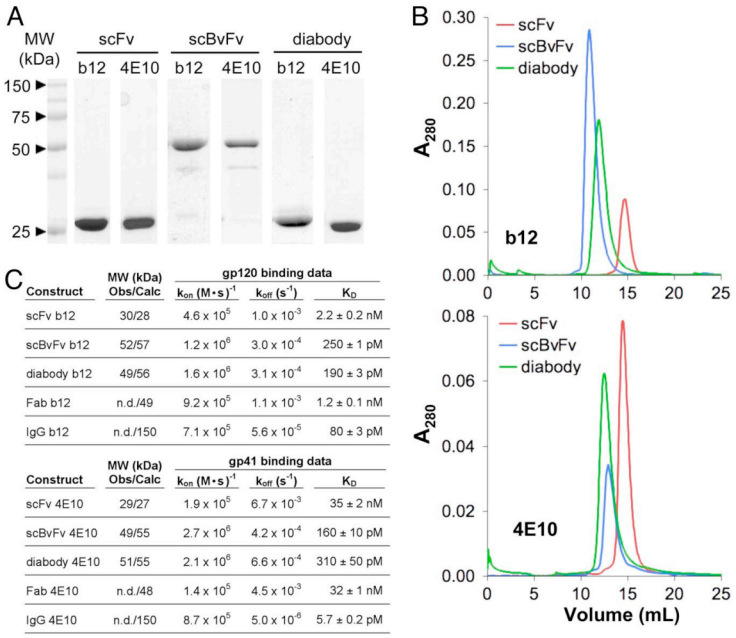

C

Construct	MW (kDa) Obs/Calc	gp120 binding data k_{on} $(M \cdot s)^{-1}$	k_{off} (s^{-1})	K_D
scFv b12	30/28	4.6×10^5	1.0×10^{-3}	2.2 ± 0.2 nM
scBvFv b12	52/57	1.2×10^6	3.0×10^{-4}	250 ± 1 pM
diabody b12	49/56	1.6×10^6	3.1×10^{-4}	190 ± 3 pM
Fab b12	n.d./49	9.2×10^5	1.1×10^{-3}	1.2 ± 0.1 nM
IgG b12	n.d./150	7.1×10^5	5.6×10^{-5}	80 ± 3 pM

Construct	MW (kDa) Obs/Calc	gp41 binding data k_{on} $(M \cdot s)^{-1}$	k_{off} (s^{-1})	K_D
scFv 4E10	29/27	1.9×10^5	6.7×10^{-3}	35 ± 2 nM
scBvFv 4E10	49/55	2.7×10^6	4.2×10^{-4}	160 ± 10 pM
diabody 4E10	51/55	2.1×10^6	6.6×10^{-4}	310 ± 50 pM
Fab 4E10	n.d./48	1.4×10^5	4.5×10^{-3}	32 ± 1 nM
IgG 4E10	n.d./150	8.7×10^5	5.0×10^{-6}	5.7 ± 0.2 pM

Fig. 2. Biophysical characterization of the antibody constructs. (*A*) Reduced SDS/PAGE. (*B*) Gel filtration profiles. (*C*) Molecular weight determinations and binding experiments. Observed results from static light scattering experiments (Obs) are presented beside molecular weights calculated from the relevant sequence (Calc) in column 2 (n.d., not done). Kinetic and equilibrium constants are presented in columns 3–5.

differences in size and flexibility contribute to the neutralization mechanisms of b12 and 4E10. Using an in vitro neutralization assay, we compared the potencies of b12 and 4E10 constructs against a panel of clade B HIV-1 strains. Our results demonstrated that avidity enhanced neutralization by IgG b12 but only weakly enhanced neutralization by IgG 4E10, and the contribution of avidity to b12-mediated neutralization was usually most apparent for strains that were relatively insensitive to monovalent b12 reagents. Moreover, we observed that flexibility and distance between the antigen-binding sites of bivalent forms of both antibodies enhanced neutralization potency and that increased size limited neutralization by 4E10 but not b12. The implications of these results on antibody escape by HIV-1 and vaccine design are discussed.

Results

Neutralizing Antibody Fragments Are Stable and Exhibit Correct Oligomerization. To systematically compare affinities and neutralization potencies as a function of size, number, and arrangement of combining sites, we produced monovalent and bivalent forms of b12 and 4E10. As monovalent forms, we produced the combining sites as Fabs and as scFvs (single chain variable fragments), in which a 15-residue flexible Gly-Ser linker was used to link the variable heavy and variable light (V_H and V_L) domains in a single polypeptide chain (25, 26) (Fig. 1). We made 3 different bivalent forms of each antibody: the traditional IgG, a single chain bivalent Fv (scBvFv), and a diabody (Fig. 1). The scBvFv was constructed by joining 2 scFv fragments with a third Gly-Ser linker, thereby forming a single polypeptide chain with 2 antibody combining sites of identical specificities (27). In this form of bivalent reagent, the 2 combining sites are expected to be free to rotate with respect to each other. The diabody form was constructed by expressing a scFv with a short linking region (28), which promoted pairing between a V_H domain and a V_L domain on separate polypeptides to form a 3D domain-swapped dimer (29). Relative to scBvFvs, diabodies are expected to be more rigid, with 2 combining sites facing in approximately opposite directions (30). In total, we produced the Fab and IgG forms of b12 and 4E10 as well as 6 different scFv-based constructs (scFv b12, scBvFv b12, diabody b12, scFv 4E10, scBvFv 4E10, and diabody 4E10).

The scFv-based proteins were purified by Ni-NTA and size-exclusion chromatography and analyzed by SDS/PAGE (Fig. 2 *A* and *B*). To verify that each of the proteins exhibited the expected oligomeric state, molecular weights were determined by in-line multiangle static light scattering coupled with size-exclusion chromatography (Fig. 2*C*). The results were consistent with the theoretical molecular weights of the scBvFvs and diabodies, which are approximately twice the molecular weight of a scFv, demonstrating that the scFvs and scBvFvs were monomeric and the diabodies were dimeric.

Bivalent b12 and 4E10 Reagents Can Bind with Avidity. The antigen binding activities of the b12 and 4E10 proteins were evaluated by using a surface plasmon resonance-based binding assay. For these experiments, we injected b12 reagents over immobilized monomeric gp120 and 4E10 reagents over immobilized gp41. During neutralization, antibodies bind to a gp120-gp41 envelope spike trimer on the surface of the virus rather than to the separated chains that can be expressed and purified for binding assays. Thus, an affinity derived from this binding assay cannot be used to deduce the affinity of an antibody for its epitope on the surface of a virus. Instead, the binding assays were used to verify that each of the reagents bound its antigen and to determine whether the bivalent constructs could cross-link immobilized antigens on the sensor surface, which would be revealed by avidity effects resulting in higher apparent affinities relative to the counterpart monovalent constructs.

Table 1. Strain-specific IC_{50} neutralization values (nM) for each antibody construct

	Antibody construct									
	b12					4E10				
Virus strain	scFv	scBvFv	diabody	Fab	IgG	scFv	scBvFv	diabody	Fab	IgG
6535.3	760 ± 280	41 ± 6	1,100 ± 200	260 ± 80	19 ± 3	14 ± 3	19 ± 3	220 ± 90	34 ± 8	5.0 ± 1.3
QH0692.42	110 ± 10	31 ± 3	48 ± 10	76 ± 10	5.6 ± 0.4	98 ± 12	130 ± 30	1,100 ± 200	220 ± 50	38 ± 4
RHPA4259.7	12 ± 1	7.5 ± 1.2	19 ± 2	11 ± 2	1.0 ± 0.2	100 ± 20	320 ± 40	680 ± 110	760 ± 200	250 ± 50
SC422661.8	57 ± 8	12 ± 2	15 ± 4	28 ± 7	3.8 ± 0.5	10 ± 1	15 ± 2	54 ± 9	28 ± 3	15 ± 3
SF162	4.9 ± 1.7	1.2 ± 0.4	4.6 ± 0.2	2.6 ± 1.0	0.26 ± 0.04	56 ± 23	90 ± 25	480 ± 190	290 ± 130	19 ± 8
THRO4156.18	110 ± 20	12 ± 2	62 ± 29	130 ± 30	4.3 ± 1.4	35 ± 3	9.3 ± 1.5	84 ± 23	42 ± 10	3.4 ± 0.8
REJO4541.67	810 ± 250	33 ± 7	680 ± 140	290 ± 100	10 ± 2	—	—	—	—	—
WITO4160.33	390 ± 120	250 ± 70	n.d.	320 ± 60	22 ± 3	—	—	—	—	—
TRJO4551.58	—	—	—	—	—	92 ± 27	170 ± 30	610 ± 130	240 ± 30	35 ± 7
TRO.11	—	—	—	—	—	8.4 ± 0.9	27 ± 3	200 ± 50	19 ± 5	3.2 ± 0.6

n.d., not done. See discussion in *SI Text*.

All of the b12 and 4E10 reagents exhibited high antigen binding affinities with equilibrium dissociation constants (K_Ds) in the nanomolar or picomolar range [Fig. 2*C* and supporting information (SI) Fig. S1]. The K_Ds for the monovalent b12 reagents (scFv and Fab) were in close agreement (2.2 nM and 1.2 nM, respectively). All of the bivalent b12 reagents bound to gp120 with higher apparent affinities: 80 pM for IgG b12, 250 pM for scBvFv b12, and 190 pM for diabody b12 (Fig. 2*C*), demonstrating that each of the bivalent constructs contained 2 functional antigen-binding sites that could cross-link adjacent immobilized antigens. The larger distance between the binding sites in an IgG compared with the binding sites in a scBvFv or diabody (Fig. 1) would be expected to lead to increased cross-linking efficiency, rationalizing the higher apparent affinity of the IgG compared with those of the scBvFv and diabody. The results obtained for the 4E10 reagents also showed an affinity enhancement for the bivalent reagents over the monovalent reagents: The scFv and Fab bound to gp41 with K_Ds of 35 nM and 32 nM, respectively, consistent with the 20 nM K_D reported for Fab 4E10 binding to a gp41-derived peptide (31), and the IgG, scBvFv, and diabody bound with apparent K_Ds of 5.7 pM, 160 pM, and 310 pM, respectively (Fig. 2*C*).

Ability to Cross-Link Epitopes on a Virus Contributes to Neutralization by b12. Pseudovirus neutralization assays were performed for antibody constructs against a panel of 10 primary virus strains from clade B (32). Eight were originally selected for evaluating IgG b12 and IgG 4E10, but we replaced TRJO4551.58 and TRO.11 with REJO4541.67 and WITO4160.33 in the b12 analyses because they were insensitive to all of the b12 reagents except IgG b12. From plots of inhibitor concentration versus percentage inhibition, we derived molar concentrations at which 50% inhibition was observed (IC_{50} values) for each potential inhibitor (Table 1 and Fig. S2). We then compared various pairs of antibody architectures by calculating the ratio of their average molar IC_{50} values across all strains (Fig. 3).

All of the b12 reagents neutralized b12-sensitive virus isolates, but the bivalent IgG and scBvFv constructs were more potent than the monovalent scFv and Fab forms: IgG b12 was an average of 34-fold more potent than scFv b12 (i.e., the average molar IC_{50} value for the scFv divided by the average value for the IgG was 34) and 17-fold more potent than Fab b12 (Fig. 3), and scBvFv b12 was an average of 6.0-fold more potent than scFv b12 and 2.9-fold more potent than Fab b12 (Fig. 3). Diabody b12,

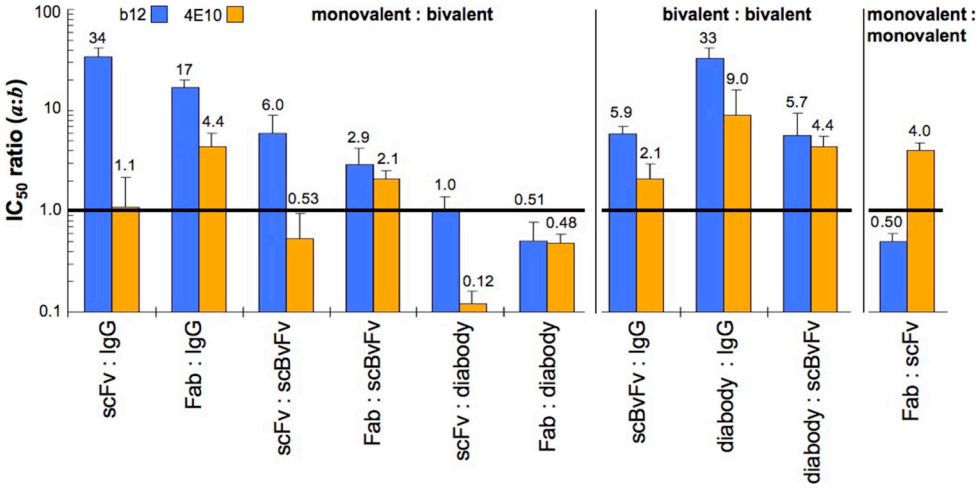

Fig. 3. Bar graph of ratios of average molar IC_{50} values (arithmetic means) for b12 constructs (blue) and 4E10 constructs (orange). Reagent pairs with an average ratio of 1.0 (black line) are equal in average potencies. Ratios >1.0 indicate that reagent *b* is more potent than reagent *a*. Ratios <1.0 indicate that reagent *a* is more potent than reagent *b*. Error bars represent the standard errors calculated from the variability in strain-specific ratios for each pair of reagents.

however, was generally indistinguishable in neutralization potency when compared with the monovalent construct (scFv/diabody average IC_{50} ratio was 1.0 and the Fab/diabody ratio was 0.51).

The increased potencies of the IgG and scBvFv forms of b12 could result from their ability to cross-link epitopes on the surface of the virus (i.e., avidity), their larger sizes or different domain structures compared with the monovalent forms, or a combination of both. None of the monovalent constructs were as large as an IgG, so the effects of size and valency could not be separated in comparisons involving the bivalent IgG architecture. However, scBvFv b12, which contains 4 domains that are comparable in size and structure to the 4 domains of monovalent Fab b12, exhibited greater neutralization potency than the Fab for all strains tested, with an average increase of 2.9-fold (Table 1 and Fig. 3). The comparison between scBvFv b12 and scFv b12 allows us to control for potential effects of domains outside the variable regions impacting affinity and specificity in binding because both constructs contain only V_L and V_H domains, yet the bivalent scBvFv b12 showed an average 6.0-fold increase in neutralization potency compared with scFv b12. We suggest that the increased potencies of the bivalent IgG and scBvFv forms of b12 relates to their abilities to cross-link epitopes on the virus, with the larger distance between combining sites in the IgG compared with the scBvFv permitting more cross-linking. Diabody b12, although bivalent and able to cross-link immobilized gp120 in a binding assay (Figs. 1 and 2*C*), was equivalent to scFv b12 in neutralization potency (Fig. 3), suggesting that the relatively rigid pairing of 2 combining sites and shorter distance between combining sites did not permit efficient cross-linking on a viral surface. Comparing scBvFv b12 with the similarly sized diabody supports the conclusion that flexibility between the antibody combining sites is important for cross-linking epitopes on a virus in b12-mediated neutralization as the scBvFv exhibited a 5.7-fold average increased potency compared with the diabody.

Neutralization by 4E10 Involves only Minimal Cross-Linking of Epitopes on a Virus. A comparison of bivalent and monovalent 4E10 constructs shows that the 4E10 bivalent reagents exhibited only modest improvements in neutralization potency compared with monovalent constructs. For example, IgG 4E10 showed a 1.1-fold and 4.4-fold improvement in potency compared with the scFv and Fab, respectively, and the scBvFv was nearly equivalent to scFv 4E10 and only slightly more potent than Fab 4E10 (Fig. 3). These results suggest that IgG 4E10 has a minimal ability to cross-link epitopes on a virus and that the flexible scBvFv 4E10 generally behaved as a monovalent reagent, as evidenced by the 0.53 scFv/scBvFv average IC_{50} ratio for 4E10 versus a ratio of 6.0 for the comparable b12 reagents. As was observed for b12, diabody 4E10 showed no increase in potency compared with the monovalent reagents (scFv/diabody average IC_{50} ratio of 0.12 and Fab/diabody average IC_{50} ratio of 0.48), demonstrating that neither diabody could efficiently cross-link epitopes on the surface of a virus.

Neutralization Potencies Suggest a Size-Restricted Epitope for 4E10, but Not b12. Comparison of IC_{50} ratios indicates that smaller and/or more flexible 4E10 reagents were generally more potent in neutralization than larger and/or less flexible reagents, a relationship that was not observed for the b12 reagents. For example, scFv 4E10 was an average of 8.3-fold more potent than the larger diabody 4E10 (average scFv/diabody IC_{50} ratio of 0.12), whereas the scFv b12 and diabody b12 were equally potent (Fig. 3). In addition, scFv 4E10 was systematically more potent than the larger Fab 4E10 (an average 4.0-fold potency increase), contrasting with scFv b12, which was 2.0-fold less potent than Fab b12 (Fig. 3 and Table 1). Indeed, the IgG 4E10 was the only reagent larger than scFv 4E10 that was also more potent, but only in 6 of the 8 strains tested (Table 1 and Table S1); for strains RHPA4259.7 and SC422661.8 the scFv was more potent than the IgG. By contrast, we observed no instances in which scFv b12 was as potent as IgG b12; the smallest difference in potencies was 12-fold with an average 34-fold difference (Fig. 3 and Table S1). These results are compatible with partial steric occlusion of the 4E10 epitope such that the larger 4E10 reagents are unable to gain complete access. Given that Fab 4E10 was found to be an average of 4.0-fold less potent than scFv 4E10, the occlusion appeared to be somewhat overcome in the case of the IgG by a modest ability to cross-link, thereby offsetting the steric penalty. In support of the hypothesis that flexibility in a 4E10 reagent improves access to the 4E10 epitope, we point to a comparison between diabody 4E10 and scBvFv 4E10, both of which were functioning as monovalent reagents during neutralization in the majority of strains tested (Table S1): Although similar in size, the more rigid diabody exhibited an average 4.4-fold weaker neutralization potency than the scBvFv. Taken together, the comparison of neutralization potencies for the IgG, Fab, diabody, and scFv forms of 4E10 and b12 suggested that the larger sizes of the IgG, Fab, scBvFv, and diabody forms of 4E10 prevented complete access to its epitope on gp41. See also Tables S2 and S3 for additional information.

Discussion

In this investigation, we asked whether alternative antibody architectures that do not naturally occur, such as a scFv, scBvFv, or diabody, could be used to further our understanding of the mechanisms by which the anti-gp120 antibody b12 and the anti-gp41 antibody 4E10 neutralize primary isolates in clade B of HIV-1. A comparative analysis of the neutralization potencies of these architectures as well as Fab and IgG forms of these antibodies yielded several conclusions that were consistent across multiple strains.

First, our analysis suggested that cross-linking HIV-1 epitopes contributes to the neutralization mechanism of IgG b12 but is less apparent for neutralization by IgG 4E10. Inefficient cross-linking by 4E10 may be related to its orientation when binding gp41: Previous reports suggested that a bound 4E10 Fab is oriented approximately perpendicular to the viral envelope (33, 34), which would require an I-shaped conformation of an IgG if both Fabs were simultaneously engaged. By contrast, b12 Fabs bind approximately parallel to the viral envelope (20), which could be achieved by a T- or Y-shaped conformation. However, although bivalency was more important for b12- than 4E10-dependent neutralization, the avidity-dependent increase in potency for b12 was limited relative to IgG/Fab comparisons of antibodies that recognize antigens on other enveloped viruses (14, 35). A potential explanation for the modest avidity-dependent increase is that only ≈10% of HIV spikes lie within the span of the 2 Fabs of an IgG (SI figure 2 in ref. 21), leaving most spikes available for only monovalent binding.

Second, the results suggested that the 4E10 epitope on gp41 is presented in a sterically constrained environment in contrast to the b12 epitope on gp120, which appeared to be fully accessible to potentially neutralizing reagents. Steric occlusion of the 4E10 epitope is consistent with the observation that a polymeric IgM version of 4E10 was significantly less potent than IgG 4E10 (36). The recent finding that 4E10 preferentially binds a fusion-intermediate conformation of gp41 (37) and that neutralization by IgG 4E10 is potentiated by the addition of a peptide that holds the trimer in a prehairpin intermediate state after attachment (38) provides additional context for interpretation of the steric occlusion effect, suggesting that the scFv and flexible scBvFv were better able to access a conformational state of the trimeric spike compared with the IgG, Fab, or diabody architectures. It is interesting to note, however, that occlusion effects were less evident for 1 of the tested strains, THRO4156.18. In this case, relative to scFv 4E10, IgG 4E10 and scBvFv 4E10 were 10-fold and 3.9-fold more potent, respectively

(Table S1), suggesting at least some ability for these bivalent architectures to mediate cross-linking. THRO4156.18 is also the only strain in which Fab 4E10 and scFv 4E10 were equally potent (Table S1). Together, these results suggest that strain THRO4156.18 might be suitable for vaccination efforts to raise 4E10-like antibodies.

Given the evidence for cross-linking by b12 reagents, we considered whether cross-linking occurred within the same spike trimer (intraspike) or between spike trimers (interspike). Analysis of a recent tomographic reconstruction of b12 Fabs bound to trimeric HIV-1 spikes on intact virions (20) suggests that intraspike cross-linking is not possible for IgG b12 or scBvFv b12 because the distance between 2 bound Fabs is greater than the span of either architecture (Fig. 1 and Fig. S3). The assumption that cross-linking is exclusively interspike allows us to address the potential for mobility of trimeric spikes on the viral surface, an issue that is relevant to the mechanisms of both antibody-mediated neutralization and fusion of the HIV-1 and host cell membranes. The low density of spikes on the surface of HIV-1 (20–23) would limit interspike cross-linking if the spikes were immobile or slow to diffuse relative to the kinetics of antibody binding. For both b12 and 4E10, we observed a greater avidity enhancement for the IgG architecture over the shorter scBvFv architecture (which span maximum distances of ≈15 and ≈11 nm, respectively; see Fig. 1), arguing in favor of a restriction to spike mobility.

The highly conserved MPER of gp41, which contains the 4E10 epitope, has long been considered an attractive target for vaccine design (39–47). Our observations of steric occlusion and inefficient cross-linking by IgG 4E10 for 7 of 8 primary isolates of clade B HIV-1 suggests that the IgG architecture is not optimal for bivalent recognition of its epitope, providing an explanation for the modest potency of 4E10 compared with other neutralizing antibodies (13). Combined with the low density of surface spikes on HIV-1, these limitations may serve as another mechanism by which HIV-1 limits neutralization by antibodies and represent an obstacle to vaccines that target the MPER. If so, IgG or scBvFv reagents with increased separation and/or flexibility between combining sites might represent a previously uncharacterized class of anti-HIV-1 reagents with increased neutralization potencies and therefore increased efficacy against HIV-1.

Materials and Methods

Affinity Determinations by Surface Plasmon Resonance. Proteins were produced (scFvs, scBvFvs, diabodies, Fabs, IgGs) or purchased (gp120, gp41) as described in *SI Text*. A Biacore 2000 biosensor system (Biacore International AB) was used to derive affinities of the b12 and 4E10 constructs for gp120 and gp41, respectively. In this assay, a protein (the "ligand") is covalently coupled to a gold–dextran layer, and association and dissociation phases for binding to injected protein (the "analyte") are measured in real time in resonance units (RU) (48, 49). The gp120 and gp41 proteins were immobilized by random primary amine coupling to a CM5 sensor chip as described in the Biacore manual. Monomeric gp120 was coupled at a density of 500 RU for experiments involving b12 constructs. gp41 was coupled at 300 RU for experiments involving scFv 4E10, scBvFv 4E10, and diabody 4E10 and at 150 RU for injections of IgG 4E10. A mock-coupled flow cell was used as a reference blank in all experiments. The surfaces were blocked with 3 5-min injections of 1 M ethanolamine (pH 8.0). After blocking, regeneration solutions of 60 mM H_3PO_4 (for gp120) or 10 mM NaOH (for gp41) were repeatedly injected in short pulses until stable baselines were observed. Next, constant concentrations of the appropriate analytes followed by regeneration solution were repeatedly injected over both surfaces to verify reproducibility. For affinity measurements, a 2-fold dilution series of each analyte was injected over the flow cells at 100 μL/min at 25 °C in 10 mM Hepes buffer (pH 7.4), 150 mM NaCl, 3 mM EDTA, and 0.005% P-20 surfactant. Blank injections of just running buffer were used for double referencing (50). The chip surface was regenerated between analyte injections with 2 12-s injections.

Primary sensorgram data were preprocessed by using the Scrubber software package (Biologic Software; www.biologic.com.au). Kinetic constants were determined by simultaneously fitting the association and dissociation phases of all curves (4 or 5 injected concentrations per construct) to a 1:1 binding model by using ClampXP (51). For IgG 4E10, association data were collected at 4 concentrations, but dissociation data were collected for 2 h at only 1 concentration and fit separately because the dissociation rate was very slow. The 1:1 binding model describes a simple bimolecular interaction, yielding single association (k_{on}) and dissociation (k_{off}) values and a macroscopic (apparent) equilibrium dissociation constant (K_D), which includes density-dependent avidity effects that arise from the ability of bivalent constructs (the IgG, scBvFvs, and diabodies) to cross-link immobilized antigens. Because we wished to evaluate the effects of multivalent binding on the apparent affinities, we did not model the data for bivalent constructs with microscopic (stepwise) binding models because these models are defined in terms of monovalent binding events and would yield microscopic (i.e., intrinsic) affinities that do not include avidity effects. Errors for the K_D values were calculated with the formula $k_{off}/k_{on}*[(\delta_{on}/k_{on})^2 + (\delta_{off}/k_{off})^2]^{1/2}$, where δ_{on} and δ_{off} denote the asymptotic standard errors of the rate constants calculated in ClampXP.

Molecular Weight Determinations by Static Light Scattering. Static light-scattering experiments were performed at 25 °C by using a Superdex 75 10/30 gel filtration column (Amersham Biosciences) equipped with a Dawn Helios light scattering photometer and an Optilab rEX refractive index detector (Wyatt Technology). Protein samples (≈350 μg) were injected in TBS at a flow rate of 0.5 mL/min. Molecular weight values were calculated by using a dn/dc value of 0.185 mL/g. All data were analyzed with ASTRA software version 5.3.1.5 (Wyatt Technology).

Analysis of Neutralization Data. In vitro neutralization assays were conducted as described in the *SI Text* and previously (1, 32, 52). Molar 50% inhibitory concentration values (IC_{50}) were calculated by fitting the inhibition data to the equation $N = 100/[1+(IC_{50}/c)^H]$, where N is the percentage of neutralization, c is the concentration of the reagent being tested, and H is the Hill coefficient (KaleidaGraph v3.6, Synergy Software) (Fig. S2). For each antibody reagent, the mean IC_{50} value across 8 viral strains was calculated as an arithmetic mean by using the formula $\Sigma a_i/8$; $i = 1, 2, \ldots, 8$, where a_i refers to the IC_{50} value for viral strain i (Fig. 3), and as a geometric mean by using the formula $(\Pi a_i)^{(1/8)}$; $i = 1, 2, \ldots, 8$ (Fig. S4). The ratio of the IC_{50} value for a reagent compared with the IC_{50} value of another reagent was calculated as the ratio of the 2 means. Our conclusions did not differ using either type of calculation.

Structure Models. Models were created by using Swiss-PDB Viewer v3.9b2 (www.expasy.org/spdbv/) (53) and rendered in MacPymol (www.pymol.org/) (54).

ACKNOWLEDGMENTS. We thank Dennis Burton (Scripps Research Institute, La Jolla, CA) for 4E10 and b12 genes; David Baltimore, Lili Yang, and Kathryn Huey-Tubman for assistance with the neutralization assay; Jost Vielmetter and the Caltech Protein Expression Center; Noreen Tiangco for preparation of Fabs; Maria Suzuki for DNA preparation; and Leo Stamatatos for critical reading of the manuscript. This work was supported by Bill and Melinda Gates Foundation Grant 38660 through the Grand Challenges in Global Health Initiative and the Collaboration for AIDS Vaccine Discovery Center.

1. Wei X, et al. (2003) Antibody neutralization and escape by HIV-1. *Nature* 422:307–312.
2. Kwong PD, et al. (1998) Structure of an HIV gp120 envelope glycoprotein in complex with the CD4 receptor and a neutralizing human antibody. *Nature* 393:648–659.
3. Labrijn AF, et al. (2003) Access of antibody molecules to the conserved coreceptor binding site on glycoprotein gp120 is sterically restricted on primary human immunodeficiency virus type 1. *J Virol* 77:10557–10565.
4. Chen B, et al. (2005) Structure of an unliganded simian immunodeficiency virus gp120 core. *Nature* 433:834–841.
5. Kwong PD, et al. (2002) HIV-1 evades antibody-mediated neutralization through conformational masking of receptor-binding sites. *Nature* 420:678–682.
6. Burton DR, Stanfield RL, Wilson IA (2005) Antibody vs. HIV in a clash of evolutionary titans. *Proc Natl Acad Sci USA* 102:14943–14948.
7. Burton DR, et al. (1994) Efficient neutralization of primary isolates of HIV-1 by a recombinant human monoclonal antibody. *Science* 266:1024–1027.
8. Barbas CF, III, et al. (1992) Recombinant human Fab fragments neutralize human type 1 immunodeficiency virus in vitro. *Proc Natl Acad Sci USA* 89:9339–9343.
9. Zwick MB, et al. (2001) Broadly neutralizing antibodies targeted to the membrane-proximal external region of human immunodeficiency virus type 1 glycoprotein gp41. *J Virol* 75:10892–10905.
10. Cardoso RM, et al. (2007) Structural basis of enhanced binding of extended and helically constrained peptide epitopes of the broadly neutralizing HIV-1 antibody 4E10. *J Mol Biol* 365:1533–1544.
11. Buchacher AR, et al. (1992) Human monoclonal antibodies against gp41 and gp120 as potential agent for passive immunization. *Vaccines* 92:191–195.

12. Muster T, et al. (1993) A conserved neutralizing epitope on gp41 of human immunodeficiency virus type 1. *J Virol* 67:6642–6647.
13. Binley JM, et al. (2004) Comprehensive cross-clade neutralization analysis of a panel of anti-human immunodeficiency virus type 1 monoclonal antibodies. *J Virol* 78:13232–13252.
14. Wu H, et al. (2005) Ultra-potent antibodies against respiratory syncytial virus: Effects of binding kinetics and binding valence on viral neutralization. *J Mol Biol* 350:126–144.
15. Icenogle J, et al. (1983) Neutralization of poliovirus by a monoclonal antibody: Kinetics and stoichiometry. *Virology* 127:412–425.
16. Cavacini LA, Emes CL, Power J, Duval M, Posner MR (1994) Effect of antibody valency on interaction with cell-surface expressed HIV-1 and viral neutralization. *J Immunol* 152:2538–2545.
17. Zhu Z, et al. (2006) Potent neutralization of Hendra and Nipah viruses by human monoclonal antibodies. *J Virol* 80:891–899.
18. Kausmally L, et al. (2004) Neutralizing human antibodies to varicella-zoster virus (VZV) derived from a VZV patient recombinant antibody library. *J Gen Virol* 85:3493–3500.
19. Janeway CA, Travers P, Walport M, Schlomchik MJ (2005) *Immunobiology* (Garland Science Publishing, New York), 6th Ed.
20. Liu J, Bartesaghi A, Borgnia MJ, Sapiro G, Subramaniam S (2008) Molecular architecture of native HIV-1 gp120 trimers. *Nature* 455:109–113.
21. Zhu P, et al. (2006) Distribution and three-dimensional structure of AIDS virus envelope spikes. *Nature* 441:847–852.
22. Sougrat R, et al. (2007) Electron tomography of the contact between T cells and SIV/HIV-1: Implications for viral entry. *PLoS Pathog* 3:e63.
23. Chertova E, et al. (2002) Envelope glycoprotein incorporation, not shedding of surface envelope glycoprotein (gp120/SU), is the primary determinant of SU content of purified human immunodeficiency virus type 1 and simian immunodeficiency virus. *J Virol* 76:5315–5325.
24. Yamaguchi M, Danev R, Nishiyama K, Sugawara K, Nagayama K (2008) Zernike phase contrast electron microscopy of ice-embedded influenza A virus. *J Struct Biol* 162:271–276.
25. Bird RE, et al. (1988) Single-chain antigen-binding proteins. *Science* 242:423–426.
26. Huston JS, et al. (1988) Protein engineering of antibody binding sites: Recovery of specific activity in an anti-digoxin single-chain Fv analogue produced in *Escherichia coli*. *Proc Natl Acad Sci USA* 85:5879–5883.
27. Mack M, Riethmuller G, Kufer P (1995) A small bispecific antibody construct expressed as a functional single-chain molecule with high tumor cell cytotoxicity. *Proc Natl Acad Sci USA* 92:7021–7025.
28. Bennett MJ, Eisenberg D (2004) The evolving role of 3D domain swapping in proteins. *Structure (London)* 12:1339–1341.
29. Holliger P, Prospero T, Winter G (1993) ''Diabodies'': Small bivalent and bispecific antibody fragments. *Proc Natl Acad Sci USA* 90:6444–6448.
30. Perisic O, Webb PA, Holliger P, Winter G, Williams RL (1994) Crystal structure of a diabody, a bivalent antibody fragment. *Structure (London)* 2:1217–1226.
31. Brunel FM, et al. (2006) Structure–function analysis of the epitope for 4E10, a broadly neutralizing human immunodeficiency virus type 1 antibody. *J Virol* 80:1680–1687.
32. Li M, et al. (2005) Human immunodeficiency virus type 1 env clones from acute and early subtype B infections for standardized assessments of vaccine-elicited neutralizing antibodies. *J Virol* 79:10108–10125.
33. Sun ZY, et al. (2008) HIV-1 Broadly neutralizing antibody extracts its epitope from a kinked gp41 ectodomain region on the viral membrane. *Immunity* 28:52–63.
34. Cardoso RM, et al. (2005) Broadly neutralizing anti-HIV antibody 4E10 recognizes a helical conformation of a highly conserved fusion-associated motif in gp41. *Immunity* 22:163–173.
35. Schofield DJ, Stephenson JR, Dimmock NJ (1997) Variations in the neutralizing and haemagglutination-inhibiting activities of five influenza A virus-specific IgGs and their antibody fragments. *J Gen Virol* 78 (Pt 10):2431–2439.
36. Kunert R, Wolbank S, Stiegler G, Weik R, Katinger H (2004) Characterization of molecular features, antigen-binding, and in vitro properties of IgG and IgM variants of 4E10, an anti-HIV type 1 neutralizing monoclonal antibody. *AIDS Res Hum Retroviruses* 20:755–762.
37. Frey G, et al. (2008) A fusion-intermediate state of HIV-1 gp41 targeted by broadly neutralizing antibodies. *Proc Natl Acad Sci USA* 105:3739–3744.
38. Gustchina E, Bewley CA, Clore GM (2008) Sequestering of the prehairpin intermediate of gp41 by peptide N36Mut(e,g) potentiates the human immunodeficiency virus type 1 neutralizing activity of monoclonal antibodies directed against the N-terminal helical repeat of gp41. *J Virol* 82:10032–10041.
39. Law M, Cardoso RM, Wilson IA, Burton DR (2007) Antigenic and immunogenic study of membrane-proximal external region-grafted gp120 antigens by a DNA prime-protein boost immunization strategy. *J Virol* 81:4272–4285.
40. Zwick MB (2005) The membrane-proximal external region of HIV-1 gp41: A vaccine target worth exploring. *AIDS* 19:1725–1737.
41. Muster T, et al. (1994) Cross-neutralizing activity against divergent human immunodeficiency virus type 1 isolates induced by the gp41 sequence ELDKWAS. *J Virol* 68:4031–4034.
42. McGaughey GB, et al. (2003) HIV-1 vaccine development: Constrained peptide immunogens show improved binding to the anti-HIV-1 gp41 MAb. *Biochemistry* 42:3214–3223.
43. Liang X, et al. (1999) Epitope insertion into variable loops of HIV-1 gp120 as a potential means to improve immunogenicity of viral envelope protein. *Vaccine* 17:2862–2872.
44. Joyce JG, et al. (2002) Enhancement of alpha-helicity in the HIV-1 inhibitory peptide DP178 leads to an increased affinity for human monoclonal antibody 2F5 but does not elicit neutralizing responses in vitro. Implications for vaccine design. *J Biol Chem* 277:45811–45820.
45. Ho J, et al. (2005) Conformational constraints imposed on a pan-neutralizing HIV-1 antibody epitope result in increased antigenicity but not neutralizing response. *Vaccine* 23:1559–1573.
46. Eckhart L, et al. (1996) Immunogenic presentation of a conserved gp41 epitope of human immunodeficiency virus type 1 on recombinant surface antigen of hepatitis B virus. *J Gen Virol* 77 (Pt 9):2001–2008.
47. Phogat S, et al. (2008) Analysis of the human immunodeficiency virus type 1 gp41 membrane proximal external region arrayed on hepatitis B surface antigen particles. *Virology* 373:72–84.
48. Fagerstam LG, Frostell-Karlsson A, Karlsson R, Persson B, Ronnberg I (1992) Biospecific interaction analysis using surface plasmon resonance detection applied to kinetic, binding site and concentration analysis. *J Chromatogr* 597:397–410.
49. Malmqvist M (1993) Biospecific interaction analysis using biosensor technology. *Nature* 361:186–187.
50. Myszka DG (1999) Improving biosensor analysis. *J Mol Recognit* 12:279–284.
51. Myszka DG, Morton TA (1998) CLAMP: A biosensor kinetic data analysis program. *Trends Biochem Sci* 23:149–150.
52. Wei X, et al. (2002) Emergence of resistant human immunodeficiency virus type 1 in patients receiving fusion inhibitor (T-20) monotherapy. *Antimicrob Agents Chemother* 46:1896–1905.
53. Guex N, Peitsch MC (1997) SWISS-MODEL and the Swiss-PdbViewer: An environment for comparative protein modeling. *Electrophoresis* 18:2714–2723.
54. DeLano WL (2008) *The PyMOL Molecular Graphics System* (DeLano Scientific, Palo Alto, CA).
55. Saphire EO, et al. (2001) Crystal structure of a neutralizing human IGG against HIV-1: A template for vaccine design. *Science* 293:1155–1159.

Supporting Information

Klein et al. 10.1073/pnas.0811427106

SI Text

Cloning, Expression, and Protein Purification. Sequences encoding variable light and heavy (V_L and V_H) domains were amplified from genes encoding the b12 and 4E10 antibodies (gifts from D. R. Burton, Scripps Research Institute, La Jolla, CA). The V_L and V_H genes were fused using a linker encoding Gly_4Ser or $(Gly_4Ser)_3$ by bridge PCR to create 6 constructs (Fig. 1). Two were the monovalent b12 and 4E10 scFvs, which were constructed by using a $(Gly_4Ser)_3$ linker, and 4 were bivalent architectures derived from scFv genes. One of the bivalent architectures was a diabody, in which a shorter linker of only one Gly_4Ser repeat between the variable domains resulted in dimerization (diabodies b12 and 4E10) through 3D domain swapping (1–3). The other bivalent architecture was a single-chain bivalent Fv (scBvFv) consisting of a first scFv (V_L joined to V_H with a $(Gly_4Ser)_3$ linker) followed by $(Gly_4Ser)_3$ and a second scFv (V_H joined to V_L with a $(Gly_4Ser)_3$ linker).

For expression of monomeric scFvs, the b12 and 4E10 scFv genes were subcloned into the pET-22b(+) vector (EMD Biosciences) and transformed into *E. coli* strain BL21(DE3). Inclusion bodies containing unfolded scFv were solubilized and refolded as described previously (4). Briefly, bacterial cultures were grown to an OD_{600} of 0.9 at 37 °C, at which point IPTG was added to 1 mM, and the cultures were incubated for an additional 4 h. Inclusion bodies were isolated by 5 rounds of sonication and centrifugation, solubilized in 7 M guanidine with 10 mM reduced glutathione and 1 mM oxidized glutathione and refolded by rapid dilution at 4 °C in 0.1 M Tris·HCl (pH 8.0), 0.4 M arginine-HCl, 10 mM reduced glutathione, and 1 mM oxidized glutathione. After concentration, refolded scFv was further purified with Ni-NTA metal affinity Sepharose (Qiagen).

The gene encoding diabody 4E10 was subcloned into the bicistronic pAc-κ-Fc vector (PROGEN Biotechnik) for expression in baculovirus-infected insect cells. Genes encoding diabody b12 and the scBvFv constructs were subcloned into pAcGP67-A (BD PharMingen). Recombinant baculoviruses were generated by cotransfection of a transfer vector with linearized Baculogold viral DNA (BD PharMingen) and used to infect High Five cells (Invitrogen). Supernatants were then concentrated, buffer-exchanged with 50 mM Tris·HCl (pH 7.4), and 150 mM NaCl (TBS), and purified over Ni-NTA Sepharose.

IgGs were transiently expressed in mammalian cells. Full-length 4E10 heavy-chain (IgG1 subclass) and light-chain (κ) genes were subcloned separately into pcDNA3.1(−) (Invitrogen) and cotransfected into HEK 293T cells (American Type Culture Collection; ATCC) using Lipofectamine 2000 (Invitrogen). Constructs encoding the heavy chain and light chain of IgG b12 in the bicistronic vector pDR12 (a gift from D. R. Burton) were also expressed by transient transfection in HEK 293T cells. To produce Fab 4E10, a truncated 4E10 heavy-chain gene (terminated after residue Thr-252) was cotransfected into EBNA cells (ATCC) along with the 4E10 light-chain gene. Fab b12 was prepared by papain digestion of IgG b12 expressed in HEK 293F cells (Invitrogen) using 25-kDa linear PEI as a transfection reagent (Polysciences). Intact IgGs were purified by protein A chromatography (Pierce Biotechnology), and Fabs were purified using goat anti-human Fab polyclonal antibody (Sigma–Aldrich) cross-linked to Protein A beads.

All proteins were further purified by size-exclusion chromatography using Superdex 75 10/30, Superdex 75 16/60, or Superdex 200 26/60 columns (Amersham Biosciences) running in TBS. The final yields for bacterially expressed proteins were 2 and 0.5 mg/L for scFv b12 and scFv 4E10, respectively. The yields for scBvFv b12, diabody b12, scBvFv 4E10, and diabody 4E10 were 2.5, 1, 1.5, 0.7, mg/L of insect cell supernatant, respectively. The yields for IgG b12, IgG 4E10, and Fab 4E10, were 6.5, 0.8, and 2.6 mg/L, respectively.

Protein concentrations were determined by absorbance at 280 nm using extinction coefficients valid for denatured protein calculated from the secreted protein sequences using the online tool PlotParam (http://ca.expasy.org/tools/protparam.html) (5). Extinction coefficients were: scFv b12, 52370 $M^{-1}cm^{-1}$; scBvFv b12, 104740 $M^{-1}cm^{-1}$; diabody b12, 104740 $M^{-1}cm^{-1}$; Fab b12, 74425 $M^{-1}cm^{-1}$; IgG b12, 232542 $M^{-1}cm^{-1}$; scFv 4E10, 47900 $M^{-1}cm^{-1}$; scBvFv 4E10, 95800 $M^{-1}cm^{-1}$; diabody 4E10, 95800 $M^{-1}cm^{-1}$; Fab 4E10, 69330 $M^{-1}cm^{-1}$; IgG 4E10, 209480 $M^{-1}cm^{-1}$. No significant differences were observed when absorbance measurements were compared for scFv proteins diluted either in guanidine-HCl to 6.0 M or in 10 mM Hepes (pH 7.4) and 150 mM NaCl. All proteins were >95% pure and stable at concentrations of 1–2 mg/mL at 4 °C for at least several weeks as assessed by unchanged gel filtration profiles.

Purified recombinant full-length gp120 (clade B, strain HxBc2) expressed in Chinese hamster ovary cells and recombinant gp41 ectodomain (clade B, strain MN) expressed in bacteria were purchased from Immunodiagnostics. The recombinant gp41 is a 25-kDa fragment expressed as a fusion protein and purified by affinity chromatography and preparative electrophoresis (product specifications for Immunodiagnostics catalog no. 1091). To validate the antigenicity of the recombinant gp41, scFv and IgG versions of 2F5, a monoclonal antibody that binds an epitope near the 4E10-binding site on gp41 (6), were injected over the gp41 surface in the binding assay, resulting in a 10 nM affinity for the scFv, comparable with the 5.3 nM affinity observed when binding to the MPER peptide from gp41 and a low picomolar apparent affinity for IgG binding to gp41. No significant binding of scFv b12 to gp41 was observed at a concentration of 1 μM.

Strain Selection for in Vitro Neutralization Assays. The following reagents were obtained through the AIDS Research and Reference Reagent Program, Division of AIDS, National Institute of Allergy and Infectious Diseases, National Institutes of Health: SVPB5, SVPB6, SVPB8, SVPB11, and SVPB12 (David Montefiori and Feng Gao); SVPB14, SVPB16, SVPB18 (B. H. Hahn and J. F. Salazar-Gonzalez); SVPB15 (B. H. Hahn and D. L. Kothe); SF162 (L. Stamatatos and C. Cheng-Mayer); SVPB17 (B. H. Hahn, X. Wei, and G. M. Shaw); $pSG3^{\Delta env}$ (John C. Kappes and Xiaoyun Wu); TZM-bl cells (John C. Kappes, Xiaoyun Wu, and Tranzyme Inc). HIV-1 pseudovirus particles from 10 pseudotyped primary virus strains [6535.3 (SVPB5), QH0692.42 (SVPB6), REJO4541.67 (SVPB16), RHPA4259.7 (SVPB14), SC422661.8 (SVPB8), SF162, THRO4156.18 (SVPB15), TRJO4551.58 (SVPB17), TRO.11 (SVPB12), and WITO4160.33 (SVPB18)] were prepared, and in vitro neutralization assays were performed as described previously (7–9).

To be able to generalize our results across an entire clade, we examined the sensitivities of various clades to both b12 and 4E10 using previously published results (10) to select appropriate strains. 4E10 neutralizes most/all strains regardless of clade, so choosing appropriate clade(s) for our comparison depended on b12, which is less broadly neutralizing. It was observed that clades A, B, C, D, AE, and BG contained at least 1 strain that was sensitive to IgG b12 (10). To be useful in our experiments

in which potentially weakly neutralizing reagents (e.g., monovalent constructs) would be tested, we estimated that a strain would need to have an $IC_{90} < 50$ μg/mL for IgG b12 in order for it to be possible for us to accurately derive an IC_{50} for a monovalent reagent. Clade B was the only clade in which a majority of strains met this criterion (Clade A: 2 of 12 strains; clade B: 19 of 29; clade C: 5 of 12; clade D: 3 of 11; clade AE: 1 of 10; clade BG: 1 of 1). We therefore chose to confine our comparative studies to clade B.

In Vitro Neutralization Assay Methods. Briefly, TZM-bl cells (8, 11, 12), a HeLa cell line expressing CD4, the HIV-1 coreceptors CCR5 and CXCR4, and Tat-responsive firefly luciferase, were infected by pseudotyped viruses, and single rounds of infection were detected as luminescence from luciferase. Each antibody reagent was tested for inhibition of infection in triplicate by preincubating 5,000 infectious viral units per well with a 3-fold dilution series of the potential inhibitor for 1 h at 37 °C. Ten thousand TZM-bl cells were then added to each well. After 48 h at 37 °C, the cells were lysed in the presence of Bright-Glo (Promega), and relative luminescence was recorded by using a Victor3 luminometer (PerkinElmer). Percent neutralization was calculated as $[1 - [(\delta - \gamma)/(\phi - \gamma)]] \times 100$, where δ is the relative luminescence observed for each sample well, γ is the background luminescence observed for cells without virus or antibody reagent, and ϕ is the maximum luminescence observed for cells with virus only.

Neutralization curves were plotted as the percentage of neutralization (y axis) versus concentration of potential inhibitor (x axis). Each data point on a neutralization curve is the mean of a triplicate measurement ± SEM. IC_{50} values were calculated as described (13). Briefly, neutralization curves were fit to the equation $N = 100/[1 + (IC_{50}/c)^H]$ where N is percent neutralization and c is the concentration of the reagent being tested, which constrains the maximum and minimum of each curve to 100% and 0% neutralization, respectively, and H represents the Hill coefficient (KaleidaGraph v3.6; Synergy Software). Fitting the data with a Hill coefficient constrained to a value of 1 does not change the results. Errors reported for the IC_{50} values in Table 1 were the asymptotic standard error calculated from nonlinear regression analyses and therefore represent the goodness-of-fit. An IC_{50} value could not be determined for diabody b12 neutralization of strain WITO4160.33 because the protein was not stable at the concentration necessary to achieve neutralization above ≈50%.

To evaluate the reproducibility of the IC_{50} values, we used either scFv b12 or IgG b12 as internal controls. When data from these multiple replicates were available, we reported the IC_{50} value in Table 1 as the average, and a representative curve is shown in Fig. S2. The error reported in Table 1 was then calculated as the product of the average IC_{50} value and the square root of the average of the sum of squares of the fractional errors from each of the replicates. The results from these multiple independent replicates are summarized in Table S2 and a comparison of our IC_{50} values with published IC_{50} values for IgG b12 and IgG 4E10 are presented in Table S3. These comparisons demonstrate that our neutralization curves yielded reproducible IC_{50} values that are in agreement with those published by others.

1. Bennett MJ, Eisenberg D (2004) The evolving role of 3D domain swapping in proteins. *Structure (London)* 12:1339–1341.
2. Perisic O, Webb PA, Holliger P, Winter G, Williams RL (1994) Crystal structure of a diabody, a bivalent antibody fragment. *Structure (London)* 2:1217–1226.
3. Holliger P, Prospero T, Winter G (1993) "Diabodies": Small bivalent and bispecific antibody fragments. *Proc Natl Acad Sci USA* 90:6444–6448.
4. Steinle A, et al. (2001) Interactions of human NKG2D with its ligands MICA, MICB, and homologs of the mouse RAE-1 protein family. *Immunogenetics* 53:279–287.
5. Gasteiger E, et al. (2005) Protein Identification and Analysis Tools on the ExPASy Server. *The Proteomics Protocols Handbook*, ed Walker JM (Humana Press, Totowa, NJ), pp 571–607.
6. Muster T, et al. (1993) A conserved neutralizing epitope on gp41 of human immunodeficiency virus type 1. *J Virol* 67:6642–6647.
7. Li M, et al. (2005) Human immunodeficiency virus type 1 env clones from acute and early subtype B infections for standardized assessments of vaccine-elicited neutralizing antibodies. *J Virol* 79:10108–10125.
8. Wei X, et al. (2002) Emergence of resistant human immunodeficiency virus type 1 in patients receiving fusion inhibitor (T-20) monotherapy. *Antimicrob Agents Chemother* 46:1896–1905.
9. Wei X, et al. (2003) Antibody neutralization and escape by HIV-1. *Nature* 422:307–312.
10. Binley JM, et al. (2004) Comprehensive cross-clade neutralization analysis of a panel of anti-human immunodeficiency virus type 1 monoclonal antibodies. *J Virol* 78:13232–13252.
11. Derdeyn CA, et al. (2000) Sensitivity of human immunodeficiency virus type 1 to the fusion inhibitor T-20 is modulated by coreceptor specificity defined by the V3 loop of gp120. *J Virol* 74:8358–8367.
12. Platt EJ, Wehrly K, Kuhmann SE, Chesebro B, Kabat D (1998) Effects of CCR5 and CD4 cell surface concentrations on infections by macrophagetropic isolates of human immunodeficiency virus type 1. *J Virol* 72:2855–2864.
13. Gustchina E, Bewley CA, Clore GM (2008) Sequestering of the prehairpin intermediate of gp41 by peptide N36Mut(e,g) potentiates the human immunodeficiency virus type 1 neutralizing activity of monoclonal antibodies directed against the N-terminal helical repeat of gp41. *J Virol* 82:10032–10041.

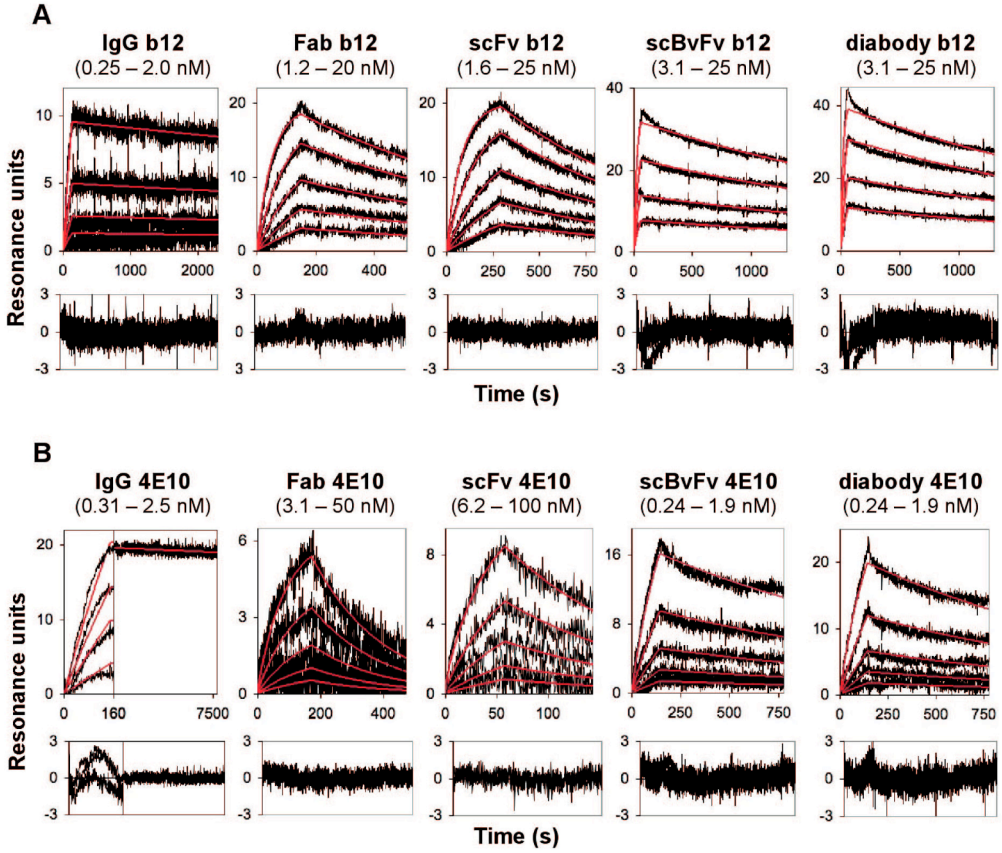

Fig. S1. Surface plasmon resonance sensorgrams for binding to immobilized antigens. Analytes were injected with the range of concentrations listed above the sensorgrams. (*A*) Sensorgrams for 2-fold dilution series of the indicated analyte binding to immobilized monomeric gp120. (*B*) Sensorgrams for 2-fold dilution series of the indicated analyte binding to immobilized gp41 ectodomain. All sensorgrams were fit with a 1-to-1 binding model. For IgG 4E10 binding to gp41, the off-rate (a concentration-independent parameter) was fit separately from the on-rate. Residual plots are shown beneath each set of fitted sensorgrams.

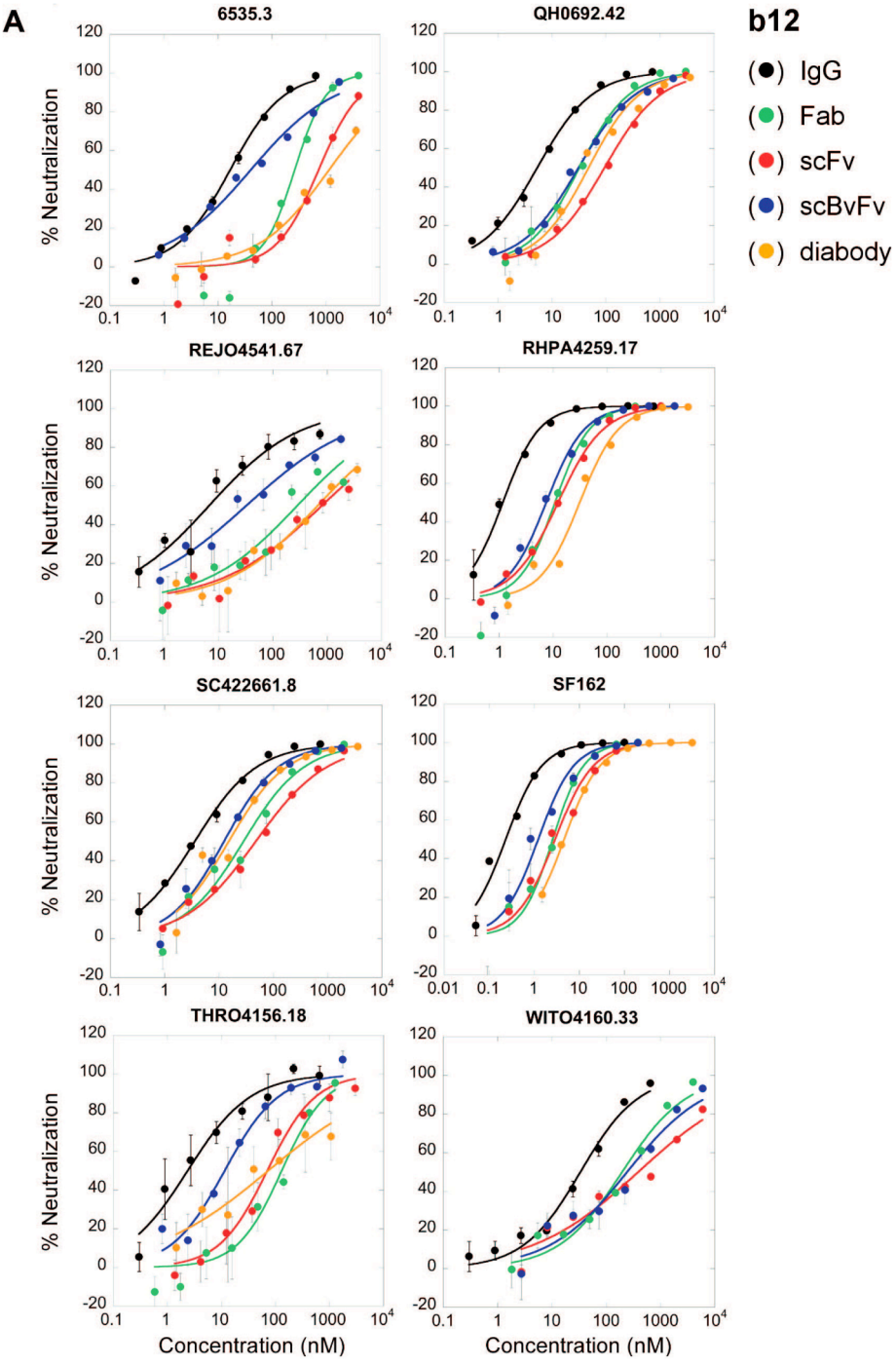

Fig. S2. In vitro pseudovirus neutralization curves. (*A*) b12 constructs.

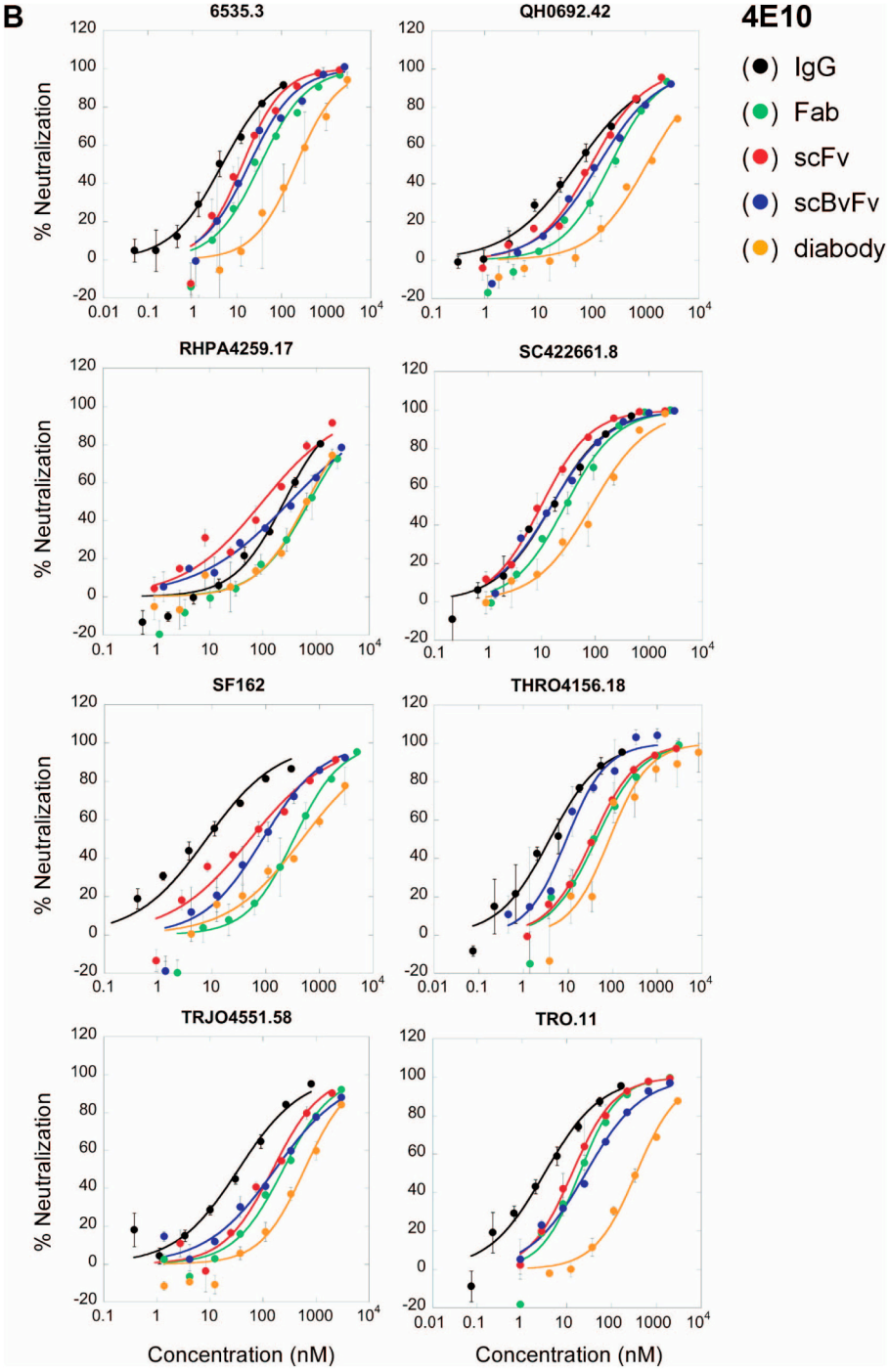

Fig. S2*B*. 4E10 constructs.

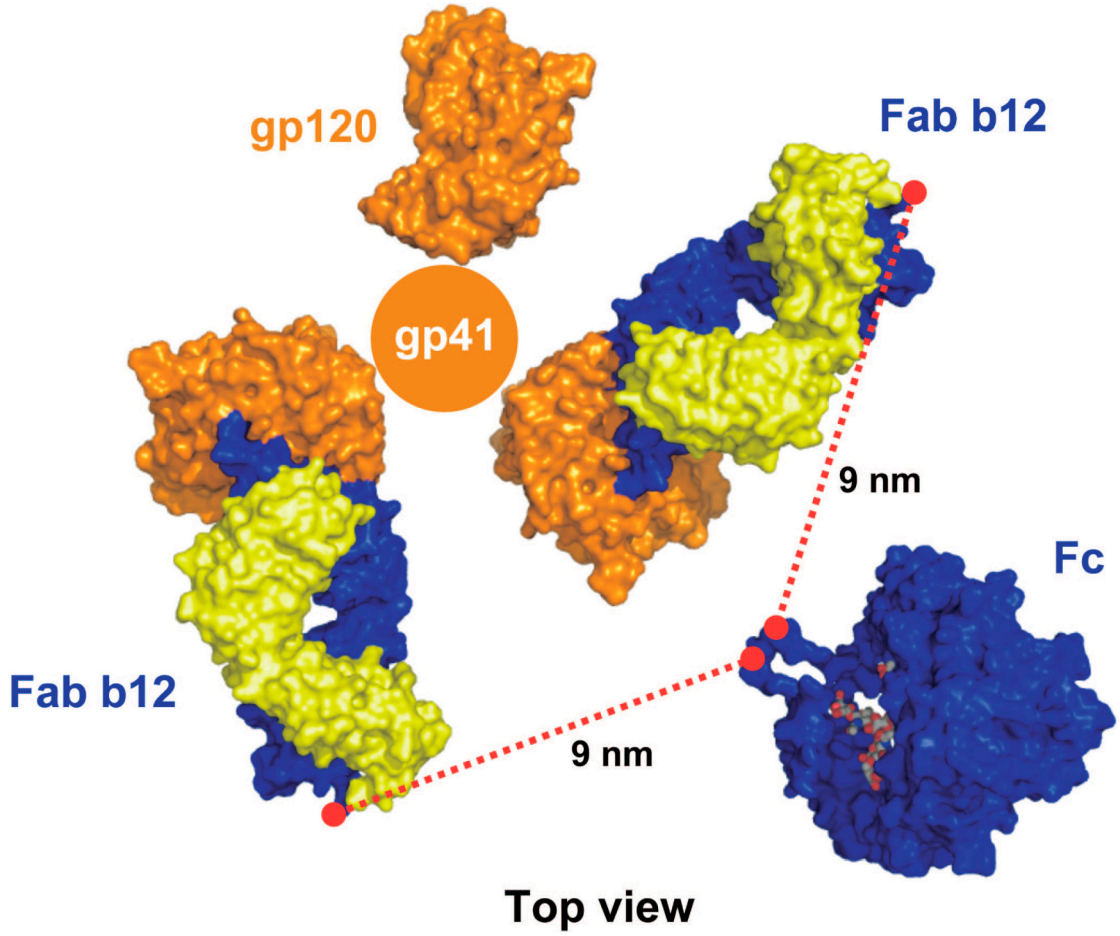

Fig. S3. Modeling of the structural requirements for IgG b12 to achieve intraspike cross-linking. Using the coordinates of the HIV gp120 trimer in its b12-bound state (orange) derived from tomographic reconstructions of intact HIV trimers (PDB ID code 3DNL) (1), we aligned the coordinates for Fab b12 (heavy chain in blue and light chain in yellow) using the crystal structure of a Fab b12/gp120 complex (PDB ID code 2NY7) (2). The Fc domain from the crystal structure of IgG b12 (PDB ID code 1HZH) (3) was then placed between and approximately equidistant from the 2 Fabs. The distance between the N-terminal Cys residue of each Fc chain (red dot) and the C-terminal Cys residue of each Fab heavy chain (red dot) is ≈9 nm, which is ≈8 nm longer than a typical IgG hinge (e.g., see IgG in Fig. 1).

1. Liu J, Bartesaghi A, Borgnia MJ, Sapiro G, Subramaniam S (2008) Molecular architecture of native HIV-1 gp120 trimers. *Nature* 455:109–113.
2. Zhou T, et al. (2007) Structural definition of a conserved neutralization epitope on HIV-1 gp120. *Nature* 445(7129):732–737.
3. Saphire EO, et al. (2001) Crystal structure of a neutralizing human IGG against HIV-1: A template for vaccine design. *Science* 293(5532):1155–1159.

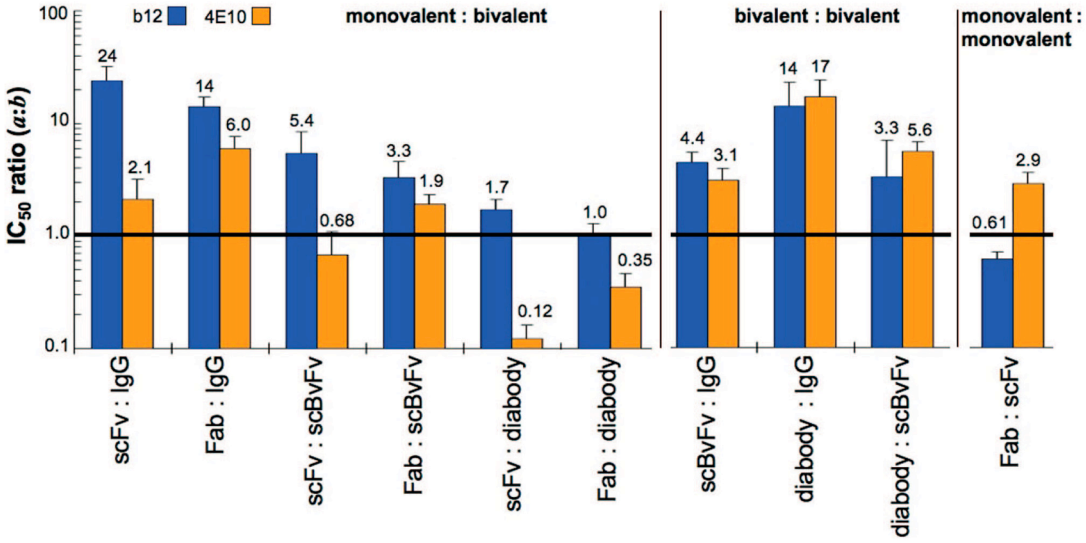

Fig. S4. Bar graph of ratios of average molar IC_{50} values (geometric means) for b12 constructs (blue) and 4E10 constructs (orange). Reagent pairs with an average ratio of 1.0 (black line) are equal in average potencies. Ratios >1.0 indicate that reagent *b* is more potent than reagent *a*. Ratios <1.0 indicate that reagent *a* is more potent than reagent *b*. Error bars represent the standard errors calculated from the variability in strain-specific ratios for each pair of reagents.

Table S1. Strain-specific IC_{50} neutralization ratios

	IC_{50} ratio by virus strain							
b12	6535.3	QH0692.42	RHPA4259.7	SC422661.8	SF162	THRO4156.18	REJO4541.67	WITO4160.33
Monovalent/bivalent								
scFv/IgG	40 ± 16	20 ± 2	12 ± 3	15 ± 3	19 ± 7	26 ± 10	81 ± 30	18 ± 6
Fab/IgG	14 ± 5	14 ± 2	11 ± 3	7.4 ± 2.1	10 ± 4	30 ± 12	29 ± 12	14 ± 3
scFv/scBvFv	19 ± 7	3.5 ± 0.5	1.6 ± 0.1	4.8 ± 1.0	4.1 ± 2.0	9.2 ± 2.3	25 ± 9	1.6 ± 0.6
Fab/scBvFv	6.3 ± 2.2	2.5 ± 0.4	1.5 ± 0.3	2.3 ± 0.7	2.2 ± 1.1	11 ± 3	8.8 ± 3.6	1.3 ± 0.4
scFv/diabody	0.69 ± 0.28	2.3 ± 0.5	0.63 ± 0.08	3.8 ± 1.1	1.1 ± 0.4	1.8 ± 0.9	1.2 ± 0.4	n.d.
Fab/diabody	0.24 ± 0.08	1.6 ± 0.4	0.58 ± 0.12	1.9 ± 0.7	0.57 ± 0.22	2.1 ± 1.1	0.43 ± 0.17	n.d.
Bivalent/bivalent								
scBvFv/IgG	2.2 ± 0.5	5.5 ± 0.7	7.5 ± 1.5	3.2 ± 0.7	4.6 ± 1.7	2.8 ± 1.0	3.3 ± 1	11 ± 3.5
diabody/IgG	58 ± 14	8.6 ± 1.9	19 ± 4.3	3.9 ± 1.2	18 ± 3	14 ± 8	68 ± 20	n.d.
diabody/scBvFv	27 ± 6	1.5 ± 0.4	2.5 ± 0.3	1.3 ± 0.4	3.8 ± 1.3	5.2 ± 2.6	21 ± 6	n.d.
Monovalent/monovalent								
Fab/scFv	0.34 ± 0.16	0.69 ± 0.11	0.92 ± 0.18	0.49 ± 0.14	0.53 ± 0.27	1.2 ± 0.3	0.36 ± 0.17	0.82 ± 0.3
4E10	6535.3	QH0692.42	RHPA4259.7	SC422661.8	SF162	THRO4156.18	TRJO4551.58	TRO.11
Monovalent/bivalent								
scFv/IgG	2.8 ± 0.9	2.6 ± 0.4	0.40 ± 0.11	0.67 ± 0.15	2.9 ± 1.7	10 ± 3	2.6 ± 0.9	2.5 ± 0.5
Fab/IgG	6.8 ± 2.4	5.8 ± 1.5	3.0 ± 1.0	1.9 ± 0.4	15 ± 9	12 ± 4	6.9 ± 1.6	5.9 ± 1.9
scFv/scBvFv	0.74 ± 0.20	0.75 ± 0.20	0.31 ± 0.07	0.67 ± 0.11	0.62 ± 0.31	3.9 ± 0.5	0.54 ± 0.19	0.30 ± 0.05
Fab/ scBvFv	1.8 ± 0.5	1.7 ± 0.5	2.4 ± 0.7	1.9 ± 0.3	3.2 ± 1.7	4.7 ± 1.2	1.4 ± 0.3	0.70 ± 0.20
scFv/diabody	0.064 ± 0.029	0.089 ± 0.020	0.15 ± 0.04	0.19 ± 0.04	0.12 ± 0.07	0.42 ± 0.12	0.15 ± 0.05	0.040 ± 0.011
Fab/diabody	0.15 ± 0.05	0.2 ± 0.06	1.1 ± 0.3	0.52 ± 0.15	0.60 ± 0.27	0.50 ± 0.26	0.39 ± 0.09	0.10 ± 0.03
Bivalent/ bivalent								
scBvFv/IgG	3.8 ± 1.2	3.4 ± 0.9	1.3 ± 0.3	1.0 ± 0.2	4.7 ± 2.4	2.6 ± 0.7	4.9 ± 1.3	8.4 ± 1.8
diabody/IgG	44 ± 21	29 ± 6	2.7 ± 0.7	3.6 ± 0.9	25 ± 15	25 ± 9	17 ± 5	63 ± 20
diabody/scBvFv	12 ± 5	8.5 ± 2.5	2.1 ± 0.4	3.6 ± 0.8	5.3 ± 2.6	9.3 ± 2.8	3.6 ± 1.0	7.4 ± 2.0
Monovalent/monovalent								
Fab/scFv	2.4 ± 0.8	2.2 ± 0.6	7.6 ± 2.5	2.8 ± 0.4	5.2 ± 3.1	1.2 ± 0.3	2.6 ± 0.8	2.4 ± 0.7

The average IC_{50} ratios presented in Fig. 3 of the main text were calculated as the ratio of their respective arithmetic mean IC_{50} values as opposed to an arithmetic mean of the individual ratios presented here. n.d., not done. See discussion in *SI Text*.

Table S2. IgG b12 and scFv b12 were used as internal controls to examine the reproducibility of independently determined IC_{50} values

	IC_{50} replicates, nM				
Isolate	1	2	3	4	Average
IgG b12					
6535.3	7.4 ± 1.4	17 ± 2	19 ± 2	34 ± 6	19 ± 3
QH0692.42	4.6 ± 0.9	5.3 ± 0.6	6.6 ± 0.3	6.7 ± 0.6	5.8 ± 0.7
RHPA4259.7	0.61 ± 0.15	1.2 ± 0.1	1.2 ± 0.1	—	1.0 ± 0.2
SC422661.8	2.1 ± 0.3	2.8 ± 0.5	3.7 ± 0.5	6.9 ± 1.3	3.9 ± 0.6
SF162	0.23 ± 0.04	0.31 ± 0.08	—	—	0.27 ± 0.06
THRO4156.18	2.3 ± 0.5	5.2 ± 1.2	5.4 ± 2.2	—	4.3 ± 1.4
scFv b12					
6535.3	410 ± 160	610 ± 340	740 ± 180	1400 ± 400	790 ± 310
QH0692.42	86 ± 17	95 ± 9	120 ± 20	130 ± 20	110 ± 20
RHPA4259.7	12 ± 1	12 ± 1	—	—	12 ± 1
SC422661.8	36 ± 8	51 ± 10	89 ± 14	—	59 ± 11
SF162	3.0 ± 1.6	4.4 ± 0.6	7.6 ± 1.4	—	5.0 ± 1.7
THRO4156.18	71 ± 10	150 ± 30	—	—	110 ± 20

Table S3. Comparison of IC_{50} values for IgG b12 and IgG 4E10 to previously published results

Isolate	Ours (μg/mL)	Li, et al. (μg/mL)*	Fold difference
IgG b12			
6535.3	2.5	1.4	1.8
QH0692.42	0.87	0.3	2.9
RHPA4259.7	0.15	0.1	1.5
SC422661.8	0.59	0.2	3.0
SF162	0.04	0.01 (0.03†)	4.1 (1.4†)
THRO4156.18	0.66	0.5	1.3
REJO4541.67	1.5	0.7	2.1
WITO4160.33	3.3	3.1	0.9
IgG 4E10			
6535.3	0.72	0.2	3.6
QH0692.42	5.5	1.4	3.9
RHPA4259.7	38	6.9	5.5
SC422661.8	1.5	0.9	1.7
SF162	2.7	0.3 (4.0†)	9.0 (0.7†)
THRO4156.18	0.51	0.3	1.7
TRJO4551.58	5.4	4.5	1.2
TRO.11	0.48	0.3	1.6

*With the exception of SF162, the HIV isolates used in our study were initially characterized in Li, et al. (1).
†Our IC_{50} values for this strain more closely match those reported by Binley, et al. (2), the laboratory in which the original characterization of this strain was conducted.

1. Li M, *et al.* (2005) Human immunodeficiency virus type 1 env clones from acute and early subtype B infections for standardized assessments of vaccine-elicited neutralizing antibodies. *J Virol* 79:10108–10125.
2. Binley JM, *et al.* (2004) Comprehensive cross-clade neutralization analysis of a panel of anti-human immunodeficiency virus type 1 monoclonal antibodies. *J Virol* 78:13232–13252.